Received: Added at production | Revised: Added at production | Accepted: Added at production

DOI: xxx/xxxx

RESEARCH ARTICLE

A Lyapunov based Saturated Super-Twisting Algorithm

Ismael Castillo*[1] | Martin Steinberger[2] | Leonid Fridman[3] | Jaime A. Moreno[4] | Martin Horn[2]

[1]Department of Applied Physics and Electronics, Umeå University, SE-901 87 Umeå, Sweden
[2]Institute of Automation and Control, Graz University of Technology, 8010 Graz, Austria
[3]Facultad de Ingeniería, Universidad Nacional Autónoma de México (UNAM), 04510 Mexico City, Mexico
[4]Instituto de Ingeniería, Universidad Nacional Autónoma de México (UNAM), 04510 Mexico City, Mexico

Correspondence
*Ismael Castillo, Email: casism@gmail.com

Present Address
Umeå University, SE-901 87 Umeå, Sweden.

Summary

Two different structures of Saturated Super-Twisting Algorithms are presented. Both structures switch between a Relay Controller and Super-Twisting Algorithm through a switching law that is based on Lyapunov level curves allowing the algorithms to generate bounded control signals. The Relay Controller works as the saturated control signal enforcing the system trajectories to reach a predefined neighborhood of the origin in which the Super-Twisting Algorithm dynamics does not saturate, ensuring finite-time convergence to the origin. In order to increase the maximal admissible bound of the perturbations, the second algorithm also includes a perturbation estimator setting Super-Twisting's integrator to the theoretically exact perturbation estimation. Experimental results are presented to validate the proposed algorithms.

KEYWORDS:
sliding mode control, saturated super-twisting algorithm, anti-windup, perturbation estimation

1 | INTRODUCTION

The Super-Twisting Algorithm[1,2] (STA) is one of the most important algorithms in sliding mode theory. It was designed to substitute a First Order Sliding Mode Controller (FOSMC) which generates a discontinuous control signal, by a continuous one. It allows the theoretically exact rejection of Lipschitz perturbations and ensures a quadratic precision of the output with respect to the sampling step due to its homogeneity properties. In addition, a second order sliding mode is achieved in finite-time, i.e. the sliding variable and its derivative are robustly driven to zero in finite-time. It has been widely used in the conventional Sliding Mode design, where systems of higher-order and non-linear dynamics can be reduced into the desired sliding dynamics of co-dimension one, i.e. a sliding variable of relative degree one, covering a wide class of systems[3,4,5,6]; and for robust exact differentiation[2] among several higher-order sliding mode differentiators[7,8].

The original version of STA, as it was introduced in Levant's Theorem 5, p.1257[1], is a saturated control law, i.e. the control signal is bounded. To ensure the saturation, the author proposed a switching strategy saturating the term of STA that is proportional to the square root of the state as well as the integral term separately. However, this switching logic can generate undesired oscillations along the saturation value as shown below.

In contrast to the original version, the most popular form of the STA[2] is given by

$$\begin{aligned} u &= -\alpha_1 |x|^{\frac{1}{2}} \operatorname{sign}(x) + z, \\ \dot{z} &= -\alpha_2 \operatorname{sign}(x). \end{aligned} \tag{1}$$

where x is the state of a first order system, and α_1, α_2, two positive constants. The first term of the control law is a nonlinear function proportional to the square root of the state while the second one is a nonlinear integral term. The STA works as a nonlinear Proportional-Integral controller leading to potentially unbounded control signals. However, in practical implementations the control effort is always limited.

It is well known[9] that the application of controllers with integral action in feedback loops with bounded control inputs lead to the so-called integral windup effect. This refers to the situation where a significant change in the set-point causes actuator saturation and as a result the error in the integral term is accumulated significantly. This leads to undesired overshoot or even to instability. Some classic anti-windup techniques make use of disabling the integral function until the variable to be controlled has entered a region where the control signal does not saturate or use additional feedback of the difference between designed and saturated control signal.

The objective of this paper is to propose two different structures of Saturated Super-Twisting Algorithms (SSTA) using an anti-windup technique in order to make the STA's control signal not to exceed predefined bounds. The contributions are:

(a) In the first SSTA, a switching law is used to combine a Relay Controller (RC) with a STA to drive the system trajectory to zero in finite-time fulfilling a saturation condition. The switching condition is designed based on a Positively Invariant Set (PINS) formed by the level curve of the Lyapunov function from Moreno et al[10] lying between the saturation curves. This approach is compared with the original STA[1] that also takes into account saturation.

(b) In comparison with Castillo et al[11], the second algorithm includes a more detailed proof where the performance of the closed loop system is improved by means of an additional perturbation estimator which takes advantage of the time intervals where the RC controller is active. Prescribed finite-time convergence gains of the estimator are obtained with the Lyapunov function from Polyakov et al[12]. This version of SSTA allows the rejection of perturbations with higher magnitude.

(c) Experiments on a real world mechanical system are carried out to illustrate the performance of the proposed STA.

The paper is organized as follows. Section 2 introduces the problem. Section 3 presents the first SSTA algorithm with a numerical example. Section 4 introduces a second algorithm using a perturbation estimator. In Section 5, experimental results for a mechanical plant are presented. Finally, Section 6 summarizes and concludes the work.

2 | PROBLEM STATEMENT

Consider the first order perturbed system

$$\dot{x} = u + \phi(t), \quad x_0 = x(0), \tag{2}$$

where $x \in \mathbb{R}$ is the state and $u \in \mathbb{R}$ the control input.

Assumption 1. The perturbation term $\phi(t)$ is a bounded and globally Lipschitz continuous function, i.e.

$$|\phi(t)| \leq \phi_{max} < \rho, \quad |\dot{\phi}(t)| \leq L. \tag{3}$$

The goal is to robustly (with respect to the perturbation) drive the state to the origin in finite-time with a saturated control signal that is continuous except at a finite number of switching instants fulfilling

$$|u(t)| \leq \rho, \tag{4}$$

where $\rho \in \mathbb{R}$ is a given constant.

3 | SATURATED SUPER TWISTING ALGORITHM

In order to guarantee boundedness of the control signal, the following dynamic switched control law[13] is proposed

$$u = \begin{cases} u_{RC} = -\rho \,\mathrm{sign}\,(x) & t < t_1 \\ \\ u_{STA} = -\alpha_1 \lceil x \rfloor^{1/2} + z & \text{else} \end{cases} \tag{5a}$$

$$\dot{z} = \begin{cases} 0 & t < t_1 \\ -\alpha_2 \mathrm{sign}\,(x) & \text{else} \end{cases} \tag{5b}$$

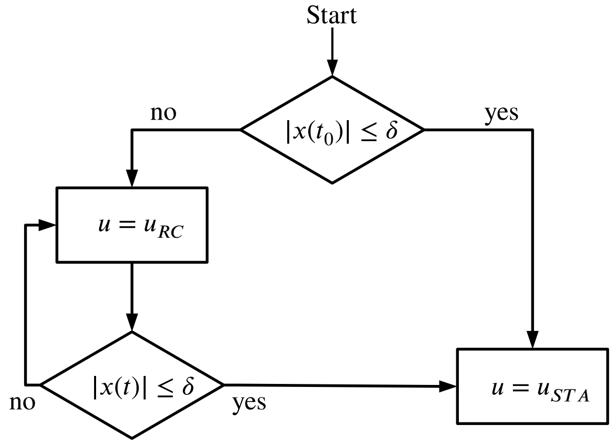

FIGURE 1 Principle of the proposed algorithm. At maximum one transition from RC to STA is possible.

where the notation $\lceil a \rfloor^b = |a|^b \text{sign}(a)$ is used and $z(t_0 = 0) = 0$. t_1 is the time instant when the trajectory of the system reaches the neighborhood $|x(t)| \leq \delta$ for the first time, i.e.

$$t_1 = \inf \left\{ t \, : \, |x(t)| \leq \delta \right\}, \tag{5c}$$

where δ is a sufficiently small positive constant to be defined later. Note that if the initial condition satisfies $|x(t_0)| \leq \delta$, $t_0 = t_1 = 0$.

The principle of the switching law is shown in Fig. 1. The RC is activated if the initial condition satisfies $|x(t_0)| > \delta$. STA is activated if the state satisfies $|x(t)| \leq \delta$ for the first time. Subsequently, STA remains activated for all future times even if $|x(t)| > \delta$.

Next, it is shown that the proposed algorithm force the trajectories to zero in finite-time fulfilling the saturation in the control input.

Theorem 1. Suppose that the perturbation $\phi(t)$ satisfies (3). Furthermore, (a) let the gains satisfy

$$\alpha_1 > 0, \; \alpha_2 > 3L + \tfrac{2L^2}{\alpha_1^2}, \tag{6}$$

(b) let the switching threshold δ be chosen such that

$$0 \leq \delta \leq \frac{2\rho^2\gamma_2}{\alpha_1^2 + 4\alpha_2}, \quad \gamma_2 = \frac{\alpha_1^2 + 8\alpha_2}{2\alpha_1^2 + 8\alpha_2}, \tag{7}$$

and (c) suppose that the maximum perturbation bound satisfies

$$\phi_{max} < \kappa\rho; \quad \kappa = \frac{2\gamma_2\rho + \sqrt{\delta}\alpha_1 - 2\sqrt{\gamma_3}}{2\rho(\gamma_2 - 1)} \tag{8}$$

where $\gamma_3 = \gamma_2\rho^2 + \delta\left(\left(\frac{\alpha_1^2}{2} + 2\alpha_2\right)(\gamma_2 - 1) + \frac{\alpha_1^2}{4}\right) + \sqrt{\delta}\gamma_2\alpha_1\rho$.
Then, all the trajectories of the closed loop system consisting of (2) and (5) converge to the origin in finite-time, and $u(t)$ fulfills (4). ▲

A sketch of proof using Lyapunov function[10] and positive invariant sets (PINS) is given in the Appendix.

Remark 1. Note that the proposed algorithm allows the trajectories of the STA to behave freely in the phase plane, i.e. even leaving the set $|x(t)| \leq \delta$ without generating high frequency switching for $x = \pm\delta$.

Note that the condition (8) is restrictive since

$$\kappa = \frac{1}{1 + \sqrt{1 + \frac{\alpha_1^2}{\alpha_1^2 + 8\alpha_2}}} < \frac{1}{2} \tag{9}$$

when $\delta = 0$. As a direct consequence, only maximal 50% of the effort in the control signal can be used to overcome perturbations.

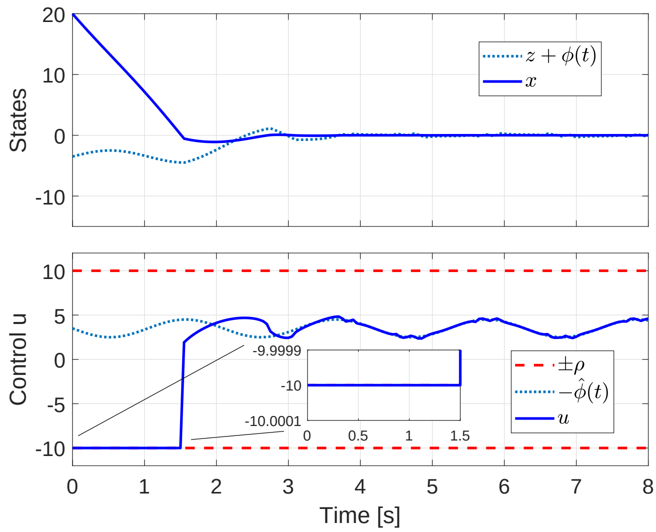

FIGURE 2 Finite-time convergence to zero of the states at the maximum rate with saturated control signal $|u| \leq \rho = 10$. Sampling step $\tau = 0.05s$.

3.1 | Example 1

Consider system (2) with the following perturbation and initial condition:

$$\phi(t) = sin(3t) - 3.5, \quad x_0 = 20.$$

The control input is saturated to $|u| \leq \rho = 10$. The gains were selected as in (6) with respect to $\phi(t)$, as $\alpha_1 = 6$ and $\alpha_2 = 10$. Choosing $\delta = 0$, the maximum allowed perturbation in (8) is $\phi_{max} = 4.66$. Note that perturbation $\phi(t)$ fulfills (8).

Fig. 2 shows how the system trajectories converge to zero in finite-time. From the initial time $t_0 = 0$ to $t_1 \approx 1.5$ the saturation of the control signal drives the state towards zero with the maximum possible rate. Then, a discontinuity in the control signal produced by the switching law occurs and a Super-Twisting Algorithm reaching phase from second 1.5 to 3.5 takes place. The trajectories converge to zero in finite-time compensating the perturbation.

The original STA [1], Theorem 5, p.1257, defined by

$$\begin{aligned} u &= u_1 + u_2, \\ \dot{u}_1 &= \begin{cases} -u & |u| > \rho \\ -\alpha \operatorname{sign}(\sigma), & |u| \leq \rho \end{cases} \\ u_2 &= \begin{cases} -\lambda |\sigma_0|^p \operatorname{sign}(\sigma) & |\sigma| > \sigma_0 \\ -\lambda |\sigma|^p \operatorname{sign}(\sigma) & |\sigma| \leq \sigma_0 \end{cases} \end{aligned}$$

was also simulated with the same gains $\lambda = \alpha_1$, $\alpha = \alpha_2$, and parameters $\rho = 10$, $\sigma_0 = 5$ and $p = \frac{1}{2}$. Results are shown in Fig. 3. Note that the saturation level is generated by high frequency switching in the control signal that can cause undesired stress in the actuator. Note also that the convergence is slightly slower.

4 | SATURATED SUPER-TWISTING WITH A PERTURBATION ESTIMATOR

In order to overcome restriction (8), an estimator of the perturbation based on Davila et al [14] is used. It is defined by

$$\begin{aligned} \dot{\hat{x}}_1 &= \beta_1 \lceil e_1 \rfloor^{1/2} - \hat{x}_2 + u \\ \dot{\hat{x}}_2 &= -\beta_2 \operatorname{sign}\left(e_1\right), \\ e_1 &= x - \hat{x}_1, \\ e_2 &= \hat{x}_2 + \phi(t), \end{aligned} \tag{10}$$

where $\hat{x}_1$ is an estimate of x_1, $\hat{x}_2$ is an estimate of $-\phi(t)$, and β_1 and β_2 positive constant gains to be designed.

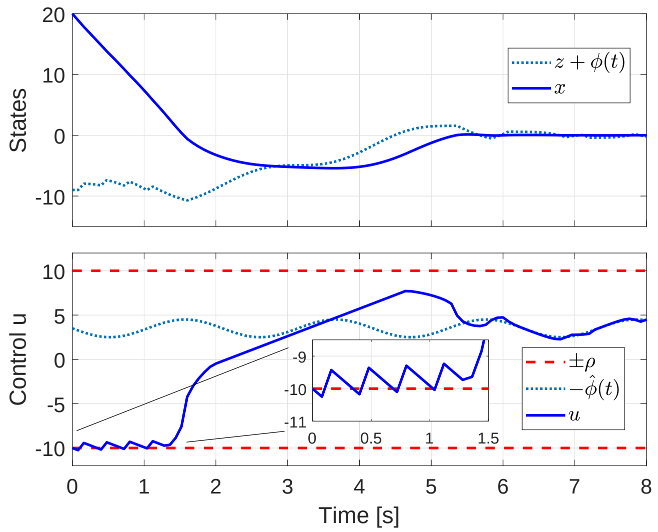

FIGURE 3 Results for the original STA from[1]. Sampling step $\tau = 0.05s$.

These estimates are used to initialize z in (5) when a switching from RC to STA at time t_1 occurs, i.e.

$$z(t_1) = \hat{x}_2(t_1) \tag{11}$$

With the appropriate selection of β_1 and β_2, the state $\hat{x}_1$ converges to x_1 and z and $\hat{x}_2$ converge to $-\phi(t)$ in finite-time T_e. The estimator has to be tuned in such a way that it is guaranteed that it converges before RC switches to STA, i.e. $T_e < t_1$.

Theorem 2. Suppose that perturbation $\phi(t)$ satisfies (3). Furthermore, (a) let the gains satisfy

$$\alpha_1 > 0, \tag{12a}$$

$$\alpha_2 > 3L + \frac{2L^2}{\alpha_1^2}, \tag{12b}$$

$$\beta_1 \geq \max\{8.8\sqrt{\tilde{L}}, 6\sqrt{2L}\}, \tag{12c}$$

$$\beta_2 \geq \max\{19\tilde{L} - 4L, 14L\} \tag{12d}$$

with

$$\tilde{L} = \frac{(\phi_{max}^2 + \rho\phi_{max})}{|x_0 - \delta|}, \tag{13}$$

for initial conditions $x_0 \neq 0$.

Then, all the trajectories of system (2) in closed-loop with (5), (10) and (11) will converge to the origin in finite-time fulfilling (4). ▲

The proof is given in the Appendix.

Remark 2. In contrast to the first algorithm presented in this paper, the second one allows one to reject perturbations with (a higher) maximal magnitude $\phi_{max} < \rho$. Nevertheless, if the initial condition is extremely close or inside of the neighborhood $|x| \leq \delta$, the perturbation estimator cannot be applied and condition (8) of Theorem 1 should be fulfilled.

Remark 3. The estimator gains (12c)-(12d) ensure the finite-time convergence of the estimator states to $e_1 = e_2 = 0$ in a time smaller than

$$T_e < T_{cmin} = \frac{|x_0 - \delta|}{\rho + \phi_{max}}. \tag{14}$$

Time T_{cmin} represents the minimum reaching time for the RC as shown in the Appendix.

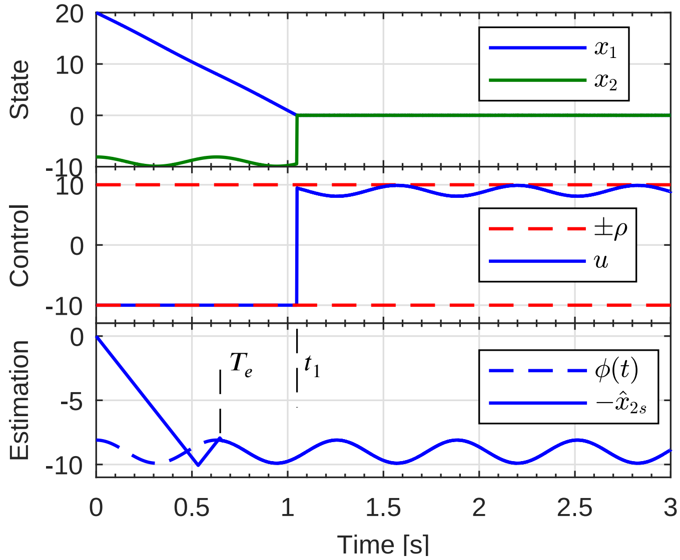

FIGURE 4 The selection of the estimator's gains as in (12c) and (12d), ensures convergence of the estimator in a finite time T_e smaller than the reaching time of the state t_1.

4.1 | Example 2

Consider system (2) with a perturbation $\phi(t) = 0.9\cos(10t) - 9$, and a saturated control input $|u| \leq \rho = 10$. According to (12a) and (12b), the controller gains are chosen as $\alpha_1 = 4$, $\alpha_2 = 37.12505$, and $\delta = 0$. Using (12c), (12d) and (13), we get $\beta_1 = 19$, and $\beta_2 = 63.5$. The estimation of the state reaching time is $T_{cmin} = \frac{|20|}{10+9.9} = 1.0050s$.

The estimation error in Fig. 4 converges to zero before second 1 ($T_e \approx 0.6s$), i.e. faster than the state converges to zero. When the state reaches $|x| = \delta = 0$ at time t_1, the STA's integrator is initialized with the exact value of the perturbation $z(t_1) = \hat{x}_{2s}(t_1) = -0.9\cos(10t_1) + 9$. Then, the trajectories are maintained in sliding mode $x = \dot{x} = 0$ for all future time with an *equivalent control* $u = -\hat{\phi}(t) = -0.9\cos(10t) + 9$. Note that the maximal perturbation $\phi_{max} = 9.9$ is near to the control limit.

5 | EXPERIMENTS

For testing the proposed algorithm, a ECP Torsional Model 205[†] is used. It consists of inertial subsystems interconnected through springs as shown in Fig. 5. Its design allows the reconfiguration of inertias, springs and the interconnection between subsystems.

Consider the problem of velocity tracking of a second-order mechanical system, i.e. second and third subsystems from above will be disconnected. Its dynamics can be represented by

$$J_m\ddot{q} + F(q,\dot{q}) = v + \omega(t), \tag{15}$$

where $q, \dot{q} \in \mathbb{R}$ are the state variables and $v \in \mathbb{R}$ the input torque which is limited by $|v| \leq \rho = 0.7Nm$. The terms in the differential equation (15) represent the moment of inertia $J_m = 0.0286kgm^2$, a bounded function F representing locally Lipschitz unknown dynamics of the system and $\omega(t)$ possibly external Lipschitz disturbances.

It is desired to realize exact velocity tracking of the trajectory $\dot{q}_d$. By defining the error variable $e_1 = \dot{q} - \dot{q}_d$, the velocity error dynamics are given by

$$\dot{e}_1 = \bar{\gamma}\Big(v + \underbrace{\omega(t) - F(q,\dot{q})}_{\phi(t)}\Big) - \ddot{q}_d, \tag{16}$$

with $\bar{\gamma} = 1/J_m$ and $\phi(t) = \omega(t) - F(q,\dot{q})$, which is a bounded locally Lipschitz perturbation. The perturbation is assumed to be bounded by a constant $|\phi(t)| \leq \phi_{max} < \rho = 0.7Nm$. Applying the control law $v = \frac{\ddot{q}_d}{\bar{\gamma}} + u$, where $u \in \mathbb{R}$ is a new control input

[†]http://www.ecpsystems.com (accessed on April 4, 2018)

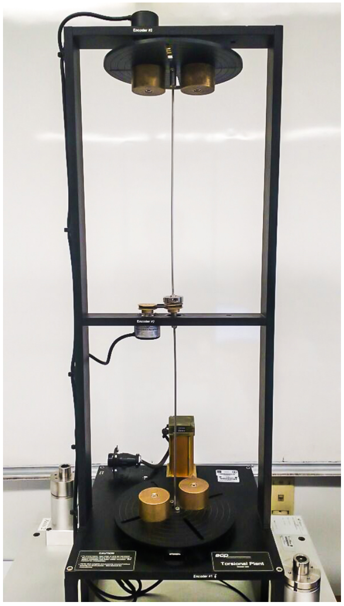

FIGURE 5 ECP Model 205: Torsional Plant.

yields

$$\dot{e}_1 = \bar{\gamma}\Big(u + \phi(t)\Big).$$

Here, we can apply the SSTA as in (5) using (11). Perturbation estimator (10) is implemented with a slight modification to take into account $\bar{\gamma}$ such that

$$\begin{aligned} \dot{\hat{x}}_1 &= \beta_1 \lceil e_1 \rfloor^{1/2} - \hat{x}_2 + \bar{\gamma}u \\ \dot{\hat{x}}_2 &= -\beta_2 \mathrm{sign}\left(e_1\right). \end{aligned} \tag{17}$$

Figure 6 shows the velocity tracking of a polynomial trajectory $\dot{q}_d$ including three steps at seconds 30, 35, and 45. A STA with a saturation function at its output without any anti-windup technique (STA+sat(u)) and no perturbation estimator in comparison with the proposed SSTA (with perturbation estimator) were applied to the plant with the same gains $\alpha_1 = 0.12$, $\alpha_2 = 0.45$, that were adjusted experimentally. The measurements clearly show overshoots, and relative errors up to 41% produced by integrator wind-up.

In contrast, the SSTA with perturbation estimator is able to reach the desired step levels without any overshoot. The corresponding control signals of experiments are depicted in Fig. 7. STA+sat(u) integrates the tracking error during all saturation intervals. On the other hand, SSTA (5) jumps from STA to RC behavior when $|u_{STA}| > \rho$ and jumps back to STA with the exact amount of integral control action to exactly compensate the dynamics and perturbations of the system avoiding the overshoot. The estimation error and the perturbation estimation are shown in Fig. 8. Video of the experiment can be found at https://youtu.be/-JIIfdY2-2s.

6 | CONCLUSIONS

Two different versions of SSTA are presented. Both versions use a dynamic switching that is based on PINS obtained from level curves of the Lyapunov function in Moreno et al [10]. RC ensures the system trajectories to reach a PINS in finite-time where the STA's continuous control signal is able to drive system trajectory to zero in finite-time fulfilling the saturation condition.

In order to increment the maximum bound of the perturbation supported by the SSTA, the second version includes a perturbation estimator allowing to set the STA's integrator to theoretically exact value of the perturbation.

Experiments were carried out using a mechanical system (see Fig. 5) that was set up as a second order system in order to illustrate the performance of the of the proposed scheme.

The proposed SSTA algorithm paves the ground for a wide use in real world applications, where saturated control is inevitable.

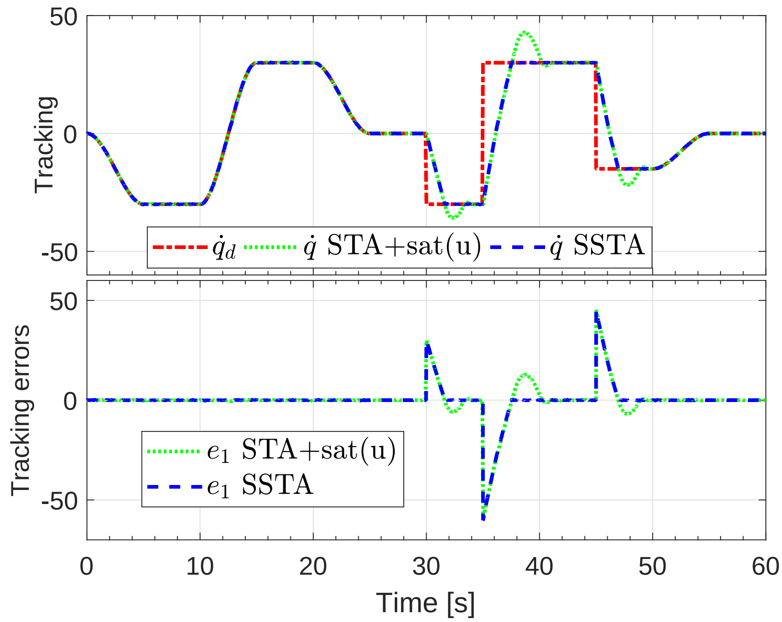

FIGURE 6 Velocity tracking of a desired polynomial trajectory $\dot{q}_d$ including three steps at second 30, 35, and 45.

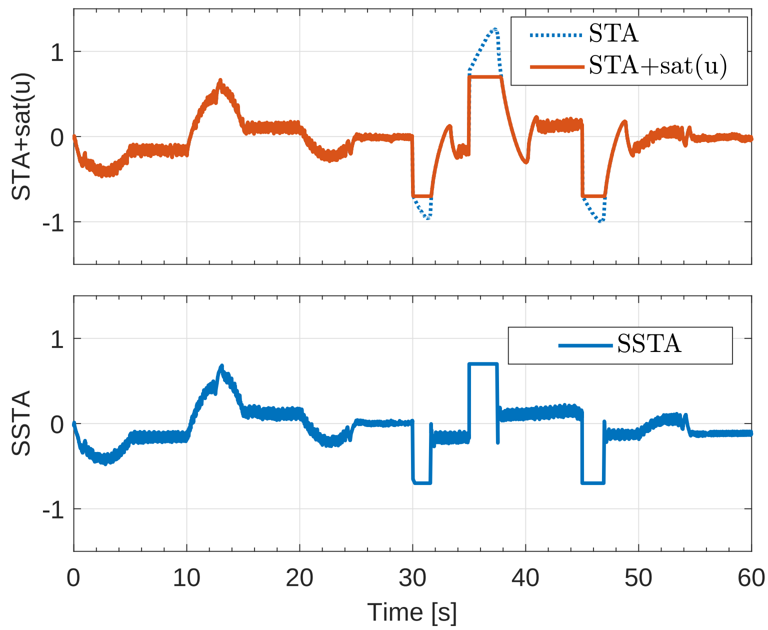

FIGURE 7 Control signals of STA+sat(u) and proposed SSTA.

How to cite this article: Castillo I., Steinberger M., Fridman L., Moreno J.A., and Horn M. (201X), A Lyapunov based Saturated Super-Twisting Algorithm, *Int J Robust Nonlinear Control*, *201X;XX:X–X*.

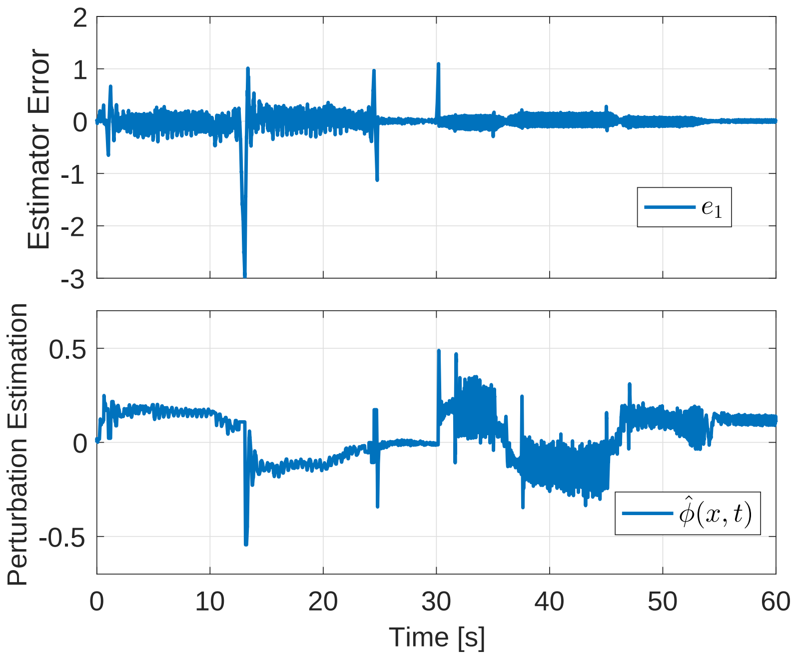

FIGURE 8 Estimation error and perturbation estimation.

APPENDIX

A SKETCH OF THE PROOF OF THEOREM 1

The next section some elements of Castillo et al [13] are shown in order to have elements for better understanding of the subsequent proof.

1. First, in [10] it is shown that if the parameters α_1 and α_2 are designed as in (6), the function,

$$V_s(x,z) = V_s(\xi_1,\xi_2) = \xi^T P \xi, \tag{A1}$$

with

$$P = \begin{bmatrix} p_{11} & -p_{12} \\ -p_{12} & p_{22} \end{bmatrix} = \frac{1}{2}\begin{bmatrix} 4\alpha_2 + \alpha_1^2 & -\alpha_1 \\ -\alpha_1 & 2 \end{bmatrix} > 0, \tag{A2}$$

and vector $\xi^T = \begin{bmatrix} \xi_1 & \xi_2 \end{bmatrix} = \begin{bmatrix} \lceil x \rfloor^{\frac{1}{2}} & z \end{bmatrix}$ is a Lyapunov function for the closed loop with the STA. It ensures the finite-time convergence of the state to the origin and the exact compensation of the perturbation.

2. The admissible range for threshold δ based on PINS for the closed loop with RC and STA is derived. The saturation of the control signal $u_{STA} = \pm\rho$ can be interpreted as the curves $z = \pm\rho + \alpha_1 \lceil x \rfloor^{\frac{1}{2}}$ in the phase plane (x, z) (see black dashed lines in Fig. A1).

3. The maximum Positive Invariant Set (PINS) contained between the two saturation curves, such that only touches the saturation curves in only one point is defined as $\Omega_s = \{\xi \in \mathbb{R}^2 | V_s \le c_s\}$,

$$c_s = \rho\gamma_2, \quad \gamma_2 = \frac{p_{11}p_{22} - p_{12}^2}{p_{22}\alpha_1^2 - 2p_{12}\alpha_1 + p_{11}} \tag{A3}$$

Then, as shown in Fig. A1(left), $V_s(x,0) = c_s$ defines the maximum value of δ such that PINS does not exceed the saturation curves.

$$V_s(x,0) = p_{11}|x| \le c_s \quad \rightarrow |x| \le \frac{c_s}{p_{11}}, \tag{A4}$$

then

$$0 \le \delta \le \frac{c_s}{p_{11}}. \tag{A5}$$

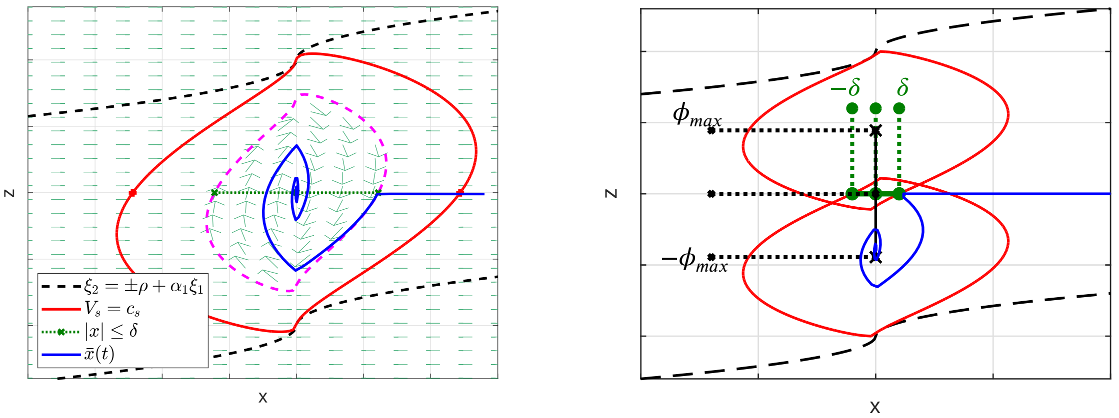

FIGURE A1 (left) Nominal Phase Plane with the maximal PINS between the saturation curves. (right) Phase Plane with perturbation $|\phi(t)| \le \phi_{max}$. Switch of control law in a neighborhood of the origin $|x| \le \delta$ (green). System trajectory (blue)

Finally with (A2) we get (7).

4. To find the maximum bound for the perturbation (8) a level curve from Lyapunov function (A2) in presence of the perturbation is evaluated in one of the saturation curves (the second curve is excluded due to symmetry), i.e. $V_s(\xi_1, \rho+\alpha_1\xi_1-\phi_{max}) = \ell_\rho$. This can be represented as a quadratic equation $a_\rho\xi_1^2 + b_\rho\xi_1 + c_\rho = 0$. Setting the discriminant $b_\rho^2 - 4a_\rho c_\rho = 0$ one can get that $\ell_\rho = (\phi_{max} - \rho)^2\gamma_2$.

5. A second level curve is evaluated at $z = 0$, i.e. $V_s(\xi_1, -\phi_{max}) = \ell_\delta$. This has two roots with respect ξ_1. Taking into account that $\xi_1 = \lceil x \rfloor^{\frac{1}{2}}$, set the minimum of the roots equals to $\sqrt{\delta}$ (i.e. $x = \delta$), and solving for ℓ_δ we get

$$\ell_\delta = \delta p_{11} + \phi_{max}^2 p_{22} + 2\phi_{max}\sqrt{\delta}p_{12}. \tag{A6}$$

6. Both conditions are obtained by setting $\ell_\rho = \ell_\delta$, and solving for ϕ_{max}, we get the maximum allowed bound for the perturbation depending on the size of the neighborhood $|x| \le \delta$, see Fig. A1(right),

$$\phi_{max} \le \kappa\rho; \quad \kappa = \frac{\gamma_2\rho + \sqrt{\delta}p_{12} - \sqrt{\gamma_3}}{\rho(\gamma_2 - p_{22})}, \tag{A7}$$

where $\gamma_3 = (p_{12}^2 + \gamma_2 p_{11} - p_{11}p_{22})\delta + 2\gamma_2 p_{12}\rho\sqrt{\delta} + \gamma_2 p_{22}\rho^2$.

7. Taking the values of the Lyapunov function (A2), we get condition (8).

8. If δ is set to zero, κ in (A7) reduces to

$$\kappa = \frac{\gamma_2\rho - \sqrt{\gamma_2\rho^2}}{\rho(\gamma_2 - 1)} = \frac{\gamma_2 - \sqrt{\gamma_2}}{(\gamma_2 - 1)} \cdot \frac{\gamma_2 + \sqrt{\gamma_2}}{\gamma_2 + \sqrt{\gamma_2}} = \frac{1}{1 + \frac{\sqrt{\gamma_2}}{\gamma_2} \cdot \frac{\sqrt{\gamma_2}}{\sqrt{\gamma_2}}} = \frac{1}{1 + \frac{1}{\sqrt{\gamma_2}}}. \tag{A8}$$

Substituting (7) in the last expression one can get

$$\kappa = \frac{1}{1 + \sqrt{1 + \frac{\alpha_1^2}{\alpha_1^2 + 8\alpha_2}}} \tag{A9}$$

which is clearly less than $\frac{1}{2}$.

B PROOF OF THEOREM 2

The proof works in two steps. First, it is shown how the estimator has to be tuned to achieve convergence before the RC switches to STA. Then, conditions for the STA parameters are derived.

The error dynamics of estimator (10) are

$$\begin{aligned}\dot{e}_1 &= -\beta_1 \lceil e_1 \rfloor^{1/2} + e_2\\ \dot{e}_2 &= -\beta_2 \text{sign}\left(e_1\right) + \dot{\phi}\end{aligned} \tag{B10}$$

with $e_2 = \hat{x}_2 + \phi(t)$. Therefore, there exists a time $T_e > 0$ where $e_1 = e_2 = 0$ as shown in [10], [12]. This implies that $\hat{x}_2 = -\phi(t)$ for all future time $t > T_e$. In the next section we design the estimator gains to make the time T_e smaller than the minimum time of convergence of the state under the Relay Controller.

The estimation of the minimum reaching time T_{cmin} of the RC is made considering the case when the perturbation helps the system trajectories to converge. Then, using the Lyapunov function

$$V_c(x) = c_1|x|,\ c_1 > 0 \tag{B11}$$

from [13] yields the time-derivative

$$\dot{V}_c(x) = -c_1\rho + c_1 sign(x)\phi(t) \tag{B12}$$

resp.

$$\min_{|\phi(t)|\leq\phi_{max}} \dot{V}_c(x) = -c_1\left(\rho + \phi_{max}\right). \tag{B13}$$

If we select $c_1 = 1/(\rho + \phi_{max})$, the Lyapunov function derivative becomes $\dot{V}_c \geq -1$ and

$$V_c(x) \geq V_c(x_0) - t = \frac{|x_0 - \delta|}{\rho + \phi_{max}} - t$$

for $t_0 = 0$. This shows that V_c reduces to zero no earlier than in time T_{cmin} given in (14).

Second, consider the Lyapunov function in Polyakov et al [12]

$$V_e(e_1, e_2) = \begin{cases} \dfrac{k^2}{4}\left(\dfrac{e_2\lceil e_1\rfloor^0}{\gamma} + k_0 e^{m(\bar{e})}\sqrt{s(\bar{e})}\right)^2 & e_1e_2 \neq 0\\ \dfrac{2\bar{k}^2e_2^2}{\beta_1^2} & e_1 = 0\\ \dfrac{|e_1|}{2} & e_2 = 0\end{cases} \tag{B14}$$

where $\bar{e} = [e_1 \quad e_2]^T$. The terms k, and k_0 depend on the state e_1 and e_2, $\bar{k}$ is a parameter to design depending on L and the gains β_1 and β_2. $s(\bar{e})$ and $m(\bar{e})$ are also non-linear functions of the state, and $g = 8\gamma/\beta_1^2$ with $\gamma(\bar{e}) := \beta_2 - L\text{sign}\left(e_1e_2\right)$.

Note that with the knowledge of the initial condition x_0 it is possible to set $\hat{x}_1(0) = x_0$, and therefore $e_1(0) = x_0 - \hat{x}_1(0) = 0$ to use the second case of (B14). We choose a parametrization of the estimator gains

$$\beta_1 = 2\sqrt{(18L + \epsilon)}, \tag{B15a}$$

$$\beta_2 = 14L + \epsilon, \tag{B15b}$$

with $\epsilon > 0$, such that the conditions of Theorem 1 [12] hold, i.e.

$$\beta_2 = 14L + \epsilon > 5L,$$

and

$$\begin{aligned}64L &< \quad \beta_1^2 \quad < 8(\beta_2 - L)\\ 64L &< (2\sqrt{18L + \epsilon})^2 < 8((14L + \epsilon) - L)\\ 64L &< \quad 72L + 4\epsilon \quad < 104L + 8\epsilon.\end{aligned}$$

Parameter g may take two possible values $g^- = 8(\beta_2 - L)/\beta_1^2, g^+ = 8(\beta_2 + L)/\beta_1^2$ depending on the values of $\gamma \in \{\beta_2 + L, \beta_2 - L\}$. Function $g = \frac{2(14L+\epsilon\pm L)}{18L+\epsilon}$ also varies depending on the selection of the parameter ϵ. Note that g is monotone with respect to ϵ since its derivative with respect to ϵ is positive, i.e.

$$\frac{dg}{d\epsilon} = \frac{2}{18L + \epsilon} - \frac{2(14L \pm L + \epsilon)}{(18L + \epsilon)^2} = \frac{2(4L \pm L)}{(18L + \epsilon)^2} > 0.$$

Therefore the limits of g^- and g^+ when $\epsilon \to 0$ and $\epsilon \to \infty$ are taken:

$$\begin{aligned} &\lim_{\epsilon\to 0} g^- = \tfrac{13}{9}, \ \lim_{\epsilon\to\infty} g^- = 2, \\ &\lim_{\epsilon\to 0} g^+ = \tfrac{15}{9}, \ \lim_{\epsilon\to\infty} g^+ = 2. \end{aligned} \tag{B16}$$

The whole range of variation of g depending on γ and ϵ is $g \in [g_m,\ g_M] = [\frac{13}{9},\ 2]$.

Parameter $\bar{k}$ should belong to a intersection set of the intervals $I(g_m) \cap I(g_M) \neq 0$, where the interval $I(g)$,

$$I(g) = \left(\frac{2}{g} + \frac{e^{(1/\sqrt{g-1})(-(\pi/2)-arctan(1/\sqrt{g-1}))}}{\sqrt{g}}, \frac{e^{(1/\sqrt{g-1})((\pi/2)-arctan(1/\sqrt{g-1}))}}{\sqrt{g}} \right). \tag{B17}$$

Evaluating the numeric endpoints of g, $I(g^-) = [1.4027,\ \ 2.01]$ and $I(g^+) = [1.0670,\ \ 1.5509]$, $\bar{k}$ can be selected as $\bar{k} = 1.4768$.

Using Theorem 1 in Polyakov et al[12], we ensure that the time derivative of (B14) along the trajectories of the system satisfies

$$\dot{V}_e \leq -k\sqrt{V_e} \leq -k_{min}\sqrt{V_e} \tag{B18}$$

and if the bound for $|e_2(0)| = |\phi(0)| = \phi_{max}$, the reaching time estimate can be referred to as

$$T_e \leq \frac{2}{k_{min}} \sqrt{V_e(0, \phi_{max})}, \tag{B19}$$

with

$$k_{min} = \frac{\beta_1}{\sqrt{8}} \min_{\substack{g\in\{g^-,g^+\} \\ \epsilon\in\{0,\infty\}}} f(g, \epsilon)$$

and

$$f(g,\epsilon) = \left| g\bar{k} - \sqrt{g} e^{\left(\frac{arctan\left(\frac{-1}{\sqrt{g-1}}\right) + \left(\frac{\pi(\beta_1^2 g - 8\beta_2)}{16L}\right)}{\sqrt{g-1}} \right)} \right|.$$

Evaluating f with the two limits g_m and g_M and the given value of L, $f(g,\epsilon) \in [f_m,\ f_M] = [0.1550,\ 2.8066]$, and $k_{min} = \frac{\beta_1}{\sqrt{8}} f_m$.

From (B14), (B19), and setting the reaching time of the estimator T_e less than the minimum reaching time of the state T_{cmin}, we have

$$T_e \leq \frac{8\bar{k}\phi_{max}}{\beta_1^2 f_m} < T_{cmin}. \tag{B20}$$

Substituting (14) in (B20) and solving for β_1 results in

$$\beta_1 \geq \sqrt{\frac{8\bar{k}}{f_m} \frac{\left(\phi_{max}^2 + \rho\phi_{max}\right)}{|x_0 - \delta|}}. \tag{B21}$$

From parametrization (B15a), we solve for ϵ such that

$$\epsilon = \frac{1}{4}\beta_1^2 - 18L. \tag{B22}$$

Substituting (B22) in parametrization (B15b) yields

$$\beta_2 = \frac{1}{4}\beta_1^2 - 4L.$$

Using the equality case of (B21) results in

$$\beta_2 \geq \frac{2\bar{k}}{f_m} \frac{\left(\phi_{max}^2 + \rho\phi_{max}\right)}{|x_0 - \delta|} - 4L. \tag{B23}$$

Note that the value of the gains β_1 and β_2 tends to zero and to $-4L$, respectively, as x_0 tends to infinity because the restriction $\epsilon > 0$ disappeared in this expressions. Therefore, conditions (B21) and (B23) are expressed as the maximum of two values to get (12c) and (12d).

As shown before and in Castillo et al[13], the PINS for STA (red lines in Fig. B2) move up or down in the (x, z)-plane depending on ϕ_{max}. In addition, they change its size depending on δ.

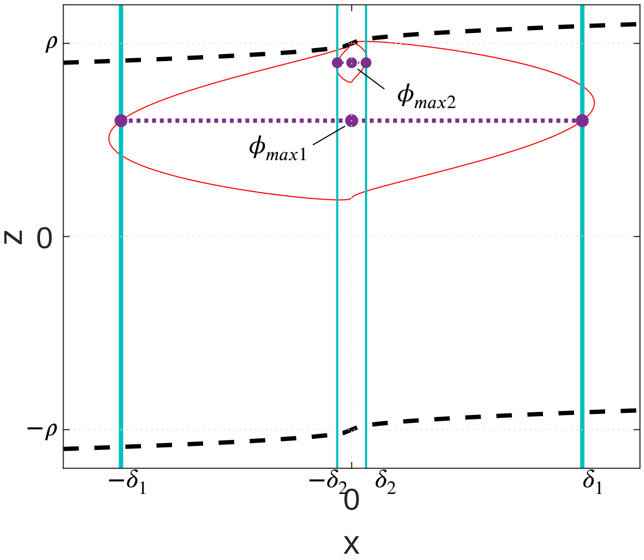

FIGURE B2 With the exact estimation of the perturbation the trajectories can start into a PINS of a size depending on δ.

With the exact estimate of the perturbation, the integral control is set to $z = -\phi(t)$ when the trajectory enters the neighborhood $|x| \leq \delta$. Following the proof in [13], we find a PINS ($\xi_2 = 0$) such that

$$V_s(\xi_1, 0) = c_\rho = (\phi_{max} - \rho)^2 \gamma_2$$

where Parameter c_ρ is related to a sublevel set that touches curve $z = \rho + \alpha_1 \xi_1$ in one point as shown in more detail in [13].

Solving for x leads to

$$|x| \leq \delta \leq \frac{(\phi_{max} - \rho)^2}{p_{11}} \gamma_2.$$

This completes the proof. ■

Note that the maximal rejectable perturbation depends on δ, i.e. the smaller δ, the bigger maximum perturbation up to $\phi_{max} = \rho$, when $\delta = 0$.

The big red region in Fig.B2 equals a PINS for the choice $\delta = \delta_1$. As a result perturbations with maximum $|\phi_{max1}|$ can be rejected. A choice of $\delta = \delta_2 < \delta_1$ gives a smaller red region as shown in Fig.B2. As a consequence, perturbations with higher magnitude $|\phi_{max2}| > |\phi_{max1}|$ can be eliminated.

References

1. Levant A. Sliding order and sliding accuracy in sliding mode control. *International Journal of Control* 1993; 58(6): 1247–1263.

2. Levant A. Robust exact differentiation via sliding mode technique. *Automatica* 1998; 34(3): 379 - 384. doi: http://dx.doi.org/10.1016/S0005-1098(97)00209-4

3. Utkin VI. *Sliding modes in control and optimization*. 116. Springer . 1992.

4. Edwards C, Spurgeon S. *Sliding mode control: theory and applications*. Crc Press . 1998.

5. Shtessel Y, Edwards C, Fridman L, Levant A. *Sliding mode control and observation*. Springer . 2014.

6. Orlov Y, Aoustin Y, Chevallereau C. Finite time stabilization of a perturbed double integrator - part I: continuous sliding mode-based output feedback synthesis. *IEEE Transactions on Automatic Control* 2011; 56(3): 614–618.

7. Polyakov A, Efimov D, Perruquetti W. Homogeneous differentiator design using implicit Lyapunov function method. In: 2014 European Control Conference (ECC). IEEE. ; 2014: 288–293.

8. Cruz-Zavala E, Moreno JA. Lyapunov Functions for Continuous and Discontinuous Differentiators. *IFAC-PapersOnLine* 2016; 49(18): 660 - 665. doi: http://dx.doi.org/10.1016/j.ifacol.2016.10.241

9. Hippe P. *Windup in control: its effects and their prevention*. Springer Science & Business Media . 2006.

10. Moreno JA, Osorio M. A Lyapunov approach to second-order sliding mode controllers and observers. In: 47th IEEE Conference on Decision and Control. IEEE. ; 2008: 2856–2861.

11. Castillo I, Steinberger M, Fridman L, Moreno J, Horn M. Saturated Super-Twisting Algorithm based on Perturbation Estimator. In: 55th Conference on Decision and Control (CDC). IEEE. ; 2016: 7325-7328

12. Polyakov A, Poznyak A. Reaching time estimation for super-twisting second order sliding mode controller via Lyapunov function designing. *IEEE Transactions on Automatic Control* 2009; 54(8): 1951–1955.

13. Castillo I, Steinberger M, Fridman L, Moreno JA, Horn M. Saturated Super-Twisting Algorithm: Lyapunov based approach. In: 14th International Workshop on Variable Structure Systems (VSS). IEEE. ; 2016: 269-273

14. Davila J, Fridman L, Poznyak A. Observation and identification of mechanical systems via second order sliding modes. *International Journal of Control* 2006; 79(10): 1251-1262. doi: 10.1080/00207170600801635